Journal of Nuclear Medicine, published on September 13, 2019 as doi:10.2967/jnumed.119.233015

Improving contrast and detectability – imaging with [^{55}Co]Co-DOTATATE in comparison with [^{64}Cu]Cu-DOTATATE and [^{68}Ga]Ga-DOTATATE

Thomas L. Andersen[1,2], Christina Baun[1], Birgitte B. Olsen[1,2], Johan H. Dam[1,2] and Helge Thisgaard[1,2,*]

1 Department of Nuclear Medicine, PET-Unit, Odense University Hospital, Odense, Denmark

2 Department of Clinical Research, University of Southern Denmark, Odense, Denmark

*Corresponding author and contact for reprints:
Helge Thisgaard (helge.thisgaard@rsyd.dk)
Department of Nuclear Medicine
Odense University Hospital
Kløvervænget 47, indg. 44-46
DK-5000 Odense C
Denmark

Word count: 4950

Disclosure

The bioimaging experiments reported in this paper were performed at DaMBIC which was established by an equipment grant from the Danish Agency for Science Technology and Innovation and by internal funding from the University of Southern Denmark. No other potential conflict of interest relevant to this article was reported.

Keywords: DOTATATE, Neuroendocrine tumor, ^{64}Cu, ^{55}Co, ^{68}Ga

Short running title**:** Imaging of metal-ion labeled DOTATATE

Abstract

PET imaging at late time points post injection (p.i.) may allow tracer clearance from normal tissue and hence improve image contrast and detectability. ^{55}Co is a promising isotope with high positron yield and a long half-life suitable for delayed time point imaging. Here, we compared the three radioconjugates [^{68}Ga]Ga-DOTATATE, [^{64}Cu]Cu-DOTATATE and [^{55}Co]Co-DOTATATE by PET/CT imaging in NOD-SCID mice bearing subcutaneous somatostatin receptor expressing AR42J tumors.

Methods: ^{55}Co and ^{64}Cu were produced by the ^{54}Fe(d,n)^{55}Co and ^{64}Ni(p,n)^{64}Cu nuclear reactions while ^{68}Ga was obtained from a ^{68}Ge/^{68}Ga generator. ^{55}Co and ^{64}Cu were labeled with DOTATATE by heating in a sodium acetate buffer and HEPES buffer, respectively. AR42J tumor-bearing mice were PET/CT scanned dynamically 0-1 h p.i. For ^{64}Cu and ^{55}Co additional late time point imaging after 4 h p.i. and 24 h p.i. were also performed. Dose calculations were performed based on a known biodistrubution. The cumulated disintegrations in each organ were calculated by integration of a fitted exponential function to the biodistribution of each respective organ. Equivalent dose calculations were hereafter calculated by OLINDA/EXM using the MIRD formalism.

Results: Tumor uptake was rapid from 0 h p.i. to 1 h p.i. for all three radioconjugates. Normal tissue ratios as represented by tumor/liver, tumor/kidney and tumor/muscle ratios increased significantly over time with [^{55}Co]Co-DOTATATE reaching the highest ratio of all radioconjugates. For [^{55}Co]Co-DOTATATE, the tumor-to-liver ratio increased to 65±16 at 4 h and 50±6 at 24 h, which were 15 ($p<0.001$) and 30 ($p<0.001$) times higher, respectively, than the corresponding ratios for [^{64}Cu]Cu-DOTATATE and 5 ($p<0.001$) times higher than that of [^{68}Ga]Ga-DOTATATE at 1 h p.i. Correspondingly, tumor/kidney and tumor/muscle ratios for [^{55}Co]Co-DOTATATE were 4 ($p<0.001$) and 11 ($p<0.001$) times higher than that of [^{64}Cu]Cu-DOTATATE at 24 h p.i. An equivalent dose was calculated to 9.6E-02 mSv/MBq for [^{55}Co]Co-DOTATATE.

Conclusions: [^{55}Co]Co-DOTATATE demonstrated superior image contrast compared to [^{64}Cu]Cu-DOTATATE and [^{68}Ga]Ga-DOTATATE for PET imaging of somatostatin receptor expressing tumors, warranting translation into clinical trials. Dosimetry calculations found

comparable effective doses for [^{55}Co]Co-DOTATATE compared to both [^{64}Cu]Cu-DOTATATE and [^{68}Ga]Ga-DOTATATE.

Introduction

Neuroendocrine tumors represent a broad heterogeneous group of malignancies. For diagnostic workup and treatment response monitoring, imaging by both functional and anatomical modalities has played a vital role. For functional molecular imaging, the somatostatin receptor (SSTR) has been found to be overexpressed in the majority of neuroendocrine tumors (NETs) (*1*) paving the way for functional imaging by targeting the somatostatin receptor. Historically, functional molecular imaging of SSTRs has been performed with Single Photon Emission Computed Tomography, SPECT, using first ^{123}I (*2*) and subsequently ^{111}In (*2,3*) and ^{99m}Tc (*4*) labelled somatostatin analogues. With the advent of Positron Emission Tomography (PET) scanners in clinical departments offering higher sensitivities and higher spatial resolution, peptides labelled with positron emitters such as ^{68}Ga, ^{18}F, ^{86}Y and ^{64}Cu have been investigated (*5-9*). Currently, ^{68}Ga has attracted most of the attention because of its positron yield of 89% and half-life of 68 min. which matches pharmacokinetics of many peptides and the readily availability from the ^{68}Ge/^{68}Ga generator where the parent isotope, ^{68}Ge, has a half-life of 270.8 days which reduces the generator exchange to 1-2 times per year. Moreover, the relative simple labeling procedure has further pushed the use of [^{68}Ga]Ga-DOTA-D-Phe1-Tyr3-Octreotide ([^{68}Ga]Ga-DOTATOC), [^{68}Ga]Ga-DOTA-D-Phe1-Tyr3-Thr8-octreotide ([^{68}Ga]Ga-DOTATATE) and [^{68}Ga]Ga-DOTA-1-Nal3-octreotide ([^{68}Ga]Ga-DOTANOC) to become the standard for functional molecular imaging in NETs. Although SSTR is the general targeted receptor the three somatostatin analogues have distinct affinity profiles for SSTR subtypes. Of these analogues, [^{68}Ga]Ga-DOTATATE exhibits the highest affinity towards somatostatin receptor subtype 2 (SSTR2) (*10*) which is the predominant subtype in NETs.

Besides development of new targeting molecules and analogues, large affinity differences have been observed in identical SSTR tracers but labeled with different isotopes (*11*). This has given rise to an increasing interest in radiotracer labeling with other radiometals than ^{68}Ga. In this respect, Reubi et al. (*12*) found half maximal inhibitory concentration (IC_{50}) of 11.7±1.7 nM and 2.5±0.5 nM of Y-DOTATOC and Ga-DOTATOC for SSTR2, respectively, while values of 1.6±0.4 nM and 0.2±0.04 nM were reported for Y-DOTATATE and Ga-DOTATATE demonstrating large affinity differences for identical vectors but different isotopes in cell lines transfected with somatostatin receptor subtypes. These results were extended by

Heppeler et al. (*13*) who synthesized and tested [^{57}Co]Co-DOTATOC as a surrogate for the positron emitting radioconjugate [^{55}Co]Co-DOTATOC and found an IC_{50} of 0.44±0.11 nM demonstrating, to our knowledge, the highest affinity seen towards SSTR2 in a AR42J tumor cell line. Further, both DOTATOC, -NOC, and -TATE have been labeled with different cobalt isotopes (^{55}Co/^{57}Co or ^{58m}Co) for theranostic applications (*14*) where the cobalt-labeled DOTATATE showed the highest translocation to the cell nucleus (*15*). Compared to [^{177}Lu]Lu-DOTATATE, [^{58m}Co]Co-DOTATATE was significantly more efficient in cell killing per cumulated decay, showing promise for a future theranostic pair using ^{55}Co/^{58m}Co.

Clinically, [^{64}Cu]Cu-DOTATATE has been introduced to overcome some of the shortcomings of [^{68}Ga]Ga-DOTA-X (*16*) such as the short half-life lowering the specific activity with time and the high β^+ energy resulting in low resolution images. In this respect [^{55}Co]Co-DOTATATE represents a promising candidate for NET imaging due to its physical half-life, allowing late time point imaging, and the high affinity for the somatostatin receptor shown for Co-DOTATOC.

The purpose of this study was to perform a head-to-head comparison of [^{55}Co]Co-DOTATATE, [^{64}Cu]Cu-DOTATATE and [^{68}Ga]Ga-DOTATATE and to characterize the *in vivo* imaging characteristics in a SSTR-positive xenografted mouse model.

Materials and Methods

Isotope production

^{68}Ga was obtained from a ^{68}Ge/^{68}Ga generator (Eckert & Ziegler) while ^{55}Co and ^{64}Cu were produced in-house using a PETtrace cyclotron. The production method for ^{55}Co has been described previously (*14,17*). Briefly, highly enriched ^{54}Fe was irradiated with 18 µA 8.4 MeV deuterons for 6 h the day before labeling followed by radiochemical separation using anion exchange resin (Dowex 1·8) and 4M HCl as eluent with further purification using a Chromafix 30-PS-HCO3 cartridge. ^{64}Cu was produced by proton bombardment of highly enriched ^{64}Ni using a fully automated solid target irradiation system (QIS, ARTMS, Canada). The irradiation was performed with 60 µA 13 MeV protons for 4 h. Following the irradiation, the target capsule was pneumatically transferred to a hotcell and mounted in a dissolution cell for dissolving the ^{64}Cu/^{64}Ni using 6 M HCl. After the dissolution process, the resulting solution

was transferred to a GE FastLab 2 Developer programmed to automatically separate the ^{64}Cu from the ^{64}Ni target material using anion exchange resin (AG 1-X8, Bio-Rad) and HCl as eluent (6.5M, 4M and 0.01M HCl).

Radiolabeling of DOTATATE

DOTATATE was purchased in GMP grade from ABX GmBH. Radiolabeling with ^{68}Ga was performed by the standard Eckert-Ziegler cassette synthesis on the Modular Lab Pharm Tracer synthesis unit in connection to the sterile GalliPharm ^{68}Ge/^{68}Ga generator. Briefly, in-house prepared kits of DOTATATE (28 nmol, ABX) in HEPES buffer (0.75 M, pH 4.0-4.1, 2 mL) were radiolabeled with ^{68}Ga at 95 °C for 400 seconds and then purified by standard C18 solid phase extraction.

Radiolabeling with ^{55}Co was performed using 4.9 nmol DOTATATE (1 µg/µl) buffered in 50 µl sodium acetate (pH 4.6, Sigma-Aldrich). This precursor solution was mixed with the [^{55}Co]$CoCl_2$ (86 MBq in 50 µl 0.04 M HCl) and heated to 90°C using dynamic PETwave microwave irradiation for 2 min.

Radiolabeling with ^{64}Cu was performed using 2.8 nmol DOTATATE (1 µg/µl) buffered in 30 µl sodium acetate (pH 4.6). This precursor solution was mixed with the [^{64}Cu]$CuCl_2$ (40 MBq in 20 µl 0.01 M HCl) and left at room temperature for 10 min. after which the solution was loaded onto an Empore cartridge (4315SD), washed with 2 mL water for injection and eluted dropwise with aqueous ethanol (70%).

All radioconjugates were finally diluted with a phosphate buffered saline containing 0.1% bovine serum albumin. After dilution a concentration of 9 vol% ethanol remained in [^{64}Cu]Cu-DOTATATE while below 2 vol% remained in [^{68}Ga]Ga-DOTATATE. No ethanol was used in the formulation of [^{55}Co]Co-DOTATATE.

Radiochemical purities were assessed using an analytical RP-HPLC (Hitachi LaChrom Elite system and a Phenomenex Jupiter C18 300A column, 150 x 4.60 mm; 5 µm) as previously described (*14*). [^{68}Ga]Ga- and [^{64}Cu]Cu-DOTATATE were further analyzed by ITLC (Biodex 150-771) and eluted in 0.1 M citric acid on which radiometals elute with the solvent front.

In vivo animal studies

Male NOD-SCID mice (n=10) of 7-9 weeks old were used from an in-house breeding program. The mice were inoculated subcutaneously with 10^6 AR42J cells in a matrigel to media ratio of 1:1 in the upper left flank. PET/CT scans were performed after confirmation of an approximately 5 mm tumor had developed as measured by an external caliper. Before scanning, the mice were anesthetized by 1.5-2% isoflurane in 100% oxygen and placed in prone position on the scanner bed. All animal experiments were approved by The Animal Experiments Inspectorate in Denmark.

PET/CT scans were performed on a preclinical Siemens Inveon PET/CT (Siemens Preclinical Solutions, Knoxville, TN, USA) scanner in docked mode. Prior to the PET data acquisition a computed tomography (CT) scan was acquired with a full 360° rotation using 270 projections acquired with 80 kV and 500 µA exposures for subsequent attenuation and scatter correction use. List mode data were reconstructed after scanning using a maximum a posteriori (MAP) algorithm in conjunction with a 3D ordered subset expectation maximum (3D OSEM) giving a central resolution of approximately 1.5 x 1.5 x 1.5 mm^3.

The injected activity was varied in the mice to match peptide amounts across all groups. Accordingly, mice were injected i.v. with activities between 1.7 MBq and 4.6 MBq corresponding to 0.12±0.02 nmol per animal. 4 mice were scanned with [^{64}Ga]Ga-DOTATATE, 3 mice with [^{64}Cu]Cu-DOTATATE and 3 mice with [^{55}Co]Co-DOTATATE.
All mice were scanned at three selected time points, namely a 0-1 h post injection (p.i.) dynamic scan, a 4 h p.i. static scan and a 24 h p.i. static scan. For [^{68}Ga]Ga-DOTATATE the 4 h p.i. and 24 h p.i. scans were omitted due to the short physical half-life of ^{68}Ga.

All mice were awakened from anesthesia between longitudinal scans and allowed to roam freely in cages with unrestricted access to food and water.

Data analysis

All PET/CT scans were analyzed in Inveon Research Workplace (IRW) software (Siemens Preclinical Solutions, Knoxville, TN, USA). Tumors were segmented by applying a fixed 40% threshold of the maximum uptake. Muscle uptake volume of interests (VOIs) was made by freehand drawing in the right anterior lower gastrocnemius muscle or alternatively in the upper left extensors in cases of high bladder uptake. Such high uptake in the bladder has a

tendency to spill into the gastrocnemius muscle making it poorly suited for a representative background uptake. Additionally, both kidneys were segmented with a procedure akin to the tumor segmentation while the liver was segmented as a freehand ellipsoidal VOI according to anatomical atlas below the lungs due to the poor soft tissue contrast on CT.

After segmentation, VOI means, standard deviations and maximum values were calculated. Furthermore, all data were decay corrected between longitudinal scans to facilitate direct comparison between different isotopes using a half-life of 12.7 h and 17.5 h for ^{64}Cu and ^{55}Co, respectively.

Dosimetry

Dosimetry calculations for [^{55}Co]Co-DOTATATE were due to animal ethics performed on the basis of a known biodistribution (*15*) published previously by our group for [^{57}Co]Co-DOTATATE. No kinetic distribution differences are expected between isotopes of the same element. The biodistribution for [^{57}Co]Co-DOTATATE is hence equal to [^{55}Co]Co-DOTATATE. The accumulated activity in the source organs, $\tilde{A}_h$, was calculated from the integration of activity in the source organs with time

$$\tilde{A}_h = \int_0^\infty A_h(t)dt$$

Source organ data was fitted by an exponential of the form

$$A_h(t) = \frac{A}{k_a - k_b} \times (e^{-k_b \cdot t} - e^{-k_a \cdot t})$$

where after the mice organ activity data were organ-to-mass scaled to human equivalents akin to a previous approach (*18*)

$$\tilde{A}_{h,o} = \tilde{A}_{a,o} \times \frac{O_{m,h}/m_h}{O_{m,a}/m_a}$$

where $\tilde{A}_{a,o}$ is the cumulated activity in the animal, $O_{m,(h,a)}$is the organ mass in a normal human (*19*) and mouse, respectively, and $m_{(h,a)}$ is the total mass of a normal human and

animal (25 g). Absorbed doses were hereafter calculated by the MIRD formalism (*20*) using *S* factors in the adult model as implemented in OLINDA/EXM 1.1 (*21*).

Statistical Analysis

Statistical analysis was performed in GraphPad Prism version 6 (GraphPad Software, La Jolla California, USA) using a two-way ANOVA with follow-up tests of either Tukey or Holm-Šídák approaches to correct for multiple comparisons.

Results

[^{68}Ga]Ga-DOTATATE was obtained in a yield of 841±159 MBq (n=6) and a radiochemical purity of 97.8±0.3% at End of Synthesis (EOS). [^{64}Cu]Cu-DOTATATE was obtained in a radiochemical and radionuclidic purity above 99% (n=1) at EOS. [^{55}Co]Co-DOTATATE was obtained in 99.5% yield and a radiochemical purity above 99.5 % (n=1) at EOS. The apparent molar activities at EOS were approximately 18, 16 and 41 MBq/nmol for [^{55}Co]Co-DOTATATE, [^{64}Cu]Cu-DOTATATE and [^{68}Ga]Ga-DOTATATE, respectively. Quantitative imaging by PET/CT showed a rapid increase in tumor uptake from 0-60 min. for all radioconjugates reaching a maximum at 1 h - 4 h p.i. The comparison of absolute uptake concentrations normalized to injected activity (IA) at 1 h p.i., 4 h p.i. and 24 h p.i. are shown in Figure 1A. No statistical significance of absolute uptake between radioconjugates at equivalent time points was found although a general lower uptake was found for [^{68}Ga]Ga-DOTATATE. Late time point imaging as made possible by the longer half-life of both ^{55}Co and ^{64}Cu compared to ^{68}Ga resulted in a higher tumor-to-kidney ratio as illustrated by Figure 1C.

Compared to 1 h p.i., the liver concentration was reduced by a factor of 9 at 24 h. p.i. for [^{55}Co]Co-DOTATATE. Oppositely, the liver concentration for [^{64}Cu]Cu-DOTATATE increased slightly, but non-significantly, from 1 h p.i. to 24 h p.i resulting in general lower tumor-to-liver ratio, cf. Figure 1B. For [^{55}Co]Co-DOTATATE, the tumor-to-liver ratio increased to 65±16 at 4 h and 50±6 at 24 h, which were 15 ($p<0.0001$) and 29 ($p<0.0001$) times higher, respectively, than the corresponding ratios for [^{64}Cu]Cu-DOTATATE and 5 ($p<0.0001$) times higher than that of [^{68}Ga]Ga-DOTATATE at 1 h p.i. Furthermore, the tumor-to-kidney ratio at 24 h p.i. for [^{55}Co]Co-DOTATATE were 4 ($p<0.0001$) times higher than the corresponding ratio for [^{64}Cu]Cu-DOTATATE and 8 ($p<0.0001$) times higher than the [^{68}Ga]Ga-DOTATATE ratio at 1 h p.i. Similarly, as a surrogate for the background uptake, the tumor-to-muscle uptake at 24 h

p.i. for [^{55}Co]Co-DOTATATE were 11 ($p<0.0001$) times higher compared to [^{64}Cu]-DOTATATE and 8 ($p<0.0001$) times higher than that of [^{68}Ga]Ga-DOTATATE ratio at 1 h p.i.

Dosimetry calculations based on [^{57}Co]Co-DOTATATE as a surrogate for [^{55}Co]Co-DOTATATE are shown in TABLE 1.

From the organ source data the effective dose equivalent was calculated to 9.6E-02 mSv/MBq with the highest individual doses given to the lungs, stomach and kidneys with 6.5E-02 mSv/MBq, 2.1E-02 mSv/MBq and 7.2E-04 mSv/MBq, respectively, cf. TABLE 1.

Discussion

Improvement in image contrast and hence detectability of malignancies from PET imaging not only depends on finding new targeting mechanisms with new tracers but also on the imaging properties of the radionuclide. The development of new tracers by combining existing targeting mechanisms, such as SSTR analogues, but with isotopes with other radiophysical properties can have a significant impact on diagnostic performance (*22,23*). Studies have shown that not only the radiophysical properties of the tracer matters for image contrast but a significant change in pharmacokinetics and affinity can also occur (*13*). In this respect ^{55}Co is a promising isotope because of its high positron yield of 75.9% (*24*) compared to only 17.6% of ^{64}Cu (*25*), its suitable half-life of 17.53 h and the demonstrated superior affinity for the somatostatin receptor subtype 2 when bound to DOTATOC (*13*) which is the predominant overexpressed subtype in NETs. Combined with the therapeutic isotope ^{58m}Co, which is a known Auger electron emitter (*17*), they constitute a promising theranostic pair. Drawbacks of ^{55}Co are the high energy γ-lines of 931.3 keV (75%), 1316 keV (7.1%) and 1408.4 keV (16.9%). These prompt gammas does not, however, influence image quality significantly on newer generation PET scanners with modern reconstructions and/or time-of-flight (*26*) and ^{55}Co is as such a viable option for clinical routine imaging with proper radiation protection.

Dosimetric calculations of [^{55}Co]Co-DOTATATE yielded an effective dose equivalent of 9.6E-02 mSv/MBq. For comparison an effective dose of 3.2E-02 mSv/MBq has been reported for [^{64}Cu]Cu-DOTATATE based on biodistributions in humans (*16*). Similarly, an effective dose of [^{68}Ga]Ga-DOTATATE of 2.1E-02 mSv/MBq has been reported (*27*). The effective dose of [^{55}Co]Co-DOTATATE is hence higher per injected activity compared to [^{64}Cu]Cu-DOTATATE

and [^{68}Ga]Ga-DOTATATE. However, the low positron yield of especially ^{64}Cu of only 17.6% requires higher amounts of administered activities to obtain diagnostic quality images. Consequently, in the study by Pfeifer et al. (*16*) a mean injected activity of 207 MBq was used. To obtain the same equivalent number of annihilation events in identical scanners, the positron fraction must be normalized between ^{64}Cu and ^{55}Co. The ratio between positron yields from ^{64}Cu and ^{55}Co is 4.2 (0.76/0.18 = 4.2) suggesting the injected activity of [^{55}Co]Co-DOTATATE should be a factor 4.2 lower compared to [^{64}Cu]Cu-DOTATATE. Scaling the mean injected activity of [^{64}Cu]Cu-DOTATATE by 4.2 results in a projected injected activity of 49 MBq [^{55}Co]Co-DOTATATE. An injected activity of 49 MBq corresponds to an effective total dose of 4.7 mSv compared to a dose commitment of 6.5 mSv of [^{64}Cu]Cu-DOTATATE from an injected dose of 207 MBq. [^{55}Co]Co-DOTATATE dosimetry is hence comparable to [^{64}Cu]Cu-DOTATATE from a patient dosimetry point of view. [^{68}Ga]Ga-DOTATATE does indeed lower the effective dose, also if adjusted to positron yield, but does, however, suffer from low contrast due to the relative higher tissue uptake and does not, due to the short physical half-life, allow for late time point imaging.

Another dosimetry aspect of ^{55}Co is the decay to ^{55}Fe which is also unstable and subsequently decays to stable ^{55}Mn with a half-life of 2.7 years. ^{55}Fe decays by electron capture with subsequent emission of low energy X-rays. The majority of iron in the body is bound to erythrocytes and is hence carried around the body with blood (*28*). It has previously been stated that ^{55}Fe could pose an additional radiation dose (*29*) after *in vivo* decay of ^{55}Co. This has, however, been disputed and a radiation dose contribution from ^{55}Fe with realistic injected activities of ^{55}Co is estimated to be around 1% of the ^{55}Co dose if all ^{55}Fe is retained in the body neglecting biological excretion. The total radiation dose from ^{55}Fe is hence believed to be negligible (*30*).

Previously, the highest known affinity for somatostatin receptor subtype 2 was found *in vitro* for [^{55}Co]Co-DOTATOC. The high affinity was not directly demonstrated in our data but a non-significant higher uptake rate from 0 h p.i. to 1 h p.i. of [^{55}Co]Co-DOTATATE compared to [^{68}Ga]Ga-DOTATATE was found supporting previous findings (*13*) suggesting that [^{55}Co]Co-DOTATATE have a higher affinity for the somatostatin receptor than [^{68}Ga]Ga-DOTATATE.

Late time point imaging to allow clearance of activity from normal tissues with [^{55}Co]Co-DOTATATE and [^{64}Cu]Cu-DOTATATE at 24 h p.i. proved very little gain from imaging at 4 h p.i. based on tumor uptake alone. For [^{64}Cu]Cu-DOTATATE a non-significant decrease on the tumor/liver ratio was observed suggesting a concentration increase of free ^{64}Cu due to [^{64}Cu]Cu-DOTATATE instability resulting in higher liver uptake with time, cf. Figure 2 D)-F). The ^{64}Cu-DOTA complex is known to transchelate *in vivo* (*31,32*) leading to activity retention in the liver (*33*) which agrees with our findings, cf. Figure 2 D)-F). On the contrary [^{55}Co]Co-DOTATATE appeared extremely stable *in vivo* with statistically significant higher ratios of tumor/liver, tumor/kidney and tumor/muscle with comparable tumor uptakes. As such, a decrease in general background was found for [^{55}Co]Co-DOTATATE over time favoring imaging at 24 h p.i. Conversely, a tumor uptake decrease over time resulted in maximum ratios of tumor/liver and tumor/muscle at 4 h p.i. Only with regard to the tumor/kidney ratio was imaging at 24 h p.i. beneficial. The very high tumor/kidney ratio at very late time point imaging opens up new possibilities for imaging of the somatostatin receptor, e.g. somatostatin receptor positive renal cell carcinomas which previously have been difficult due to the high kidney and bladder uptake with normal excretion (*34-36*).

Conclusion

The somatostatin analogue [^{55}Co]Co-DOTATATE is a promising tracer for PET imaging of SSTR-expressing tumors. The fast clearance of [^{55}Co]Co-DOTATATE from normal tissues resulted in significantly higher tumor-to-background ratios compared to what was observed for [^{64}Cu]Cu-DOTATATE and [^{68}Ga]Ga-DOTATATE. Importantly, from 4 h p.i. the uptake of [^{55}Co]Co-DOTATATE in the tumor was at least 50 times higher than the uptake in the liver, which is a major site of metastasis for NETs. Thus, [^{55}Co]Co-DOTATATE provides excellent image contrast and warrants further development for translation into the clinic.

Disclosure

The bioimaging experiments reported in this paper were performed at DaMBIC, a bioimaging research core facility at the University of Southern Denmark. DaMBIC was established by an equipment grant from the Danish Agency for Science Technology and Innovation and by

internal funding from the University of Southern Denmark. No other potential conflict of interest relevant to this article was reported.

Key Points

Question: Can [^{55}Co]Co-DOTATATE improve PET/CT image contrast by delayed imaging compared to [^{64}Cu]Cu-DOTATATE and [^{68}Ga]Ga-DOTATATE in somatostatin positive tumors?

Pertinent findings: [^{55}Co]Co-DOTATATE statistically significant improves image contrast in NOD-SCID mice bearing subcutaneous somatostatin receptor expressing AR42J tumors as exemplified by the tumor/liver, tumor/kidney and tumor/ muscle ratios. Delayed imaging with [^{55}Co]Co-DOTATATE hence offers superior image contrast compared to both [^{68}Ga]Ga-DOTATATE and [^{64}Cu]Cu-DOTATATE.

Implications for patient care: The results warrants further translation into clinical practice and holds promise for improved patient diagnostics and future applications for delayed PET/CT imaging.

References

1. Rufini V, Calcagni ML, Baum RP. Imaging of neuroendocrine tumors. *Seminars in Nuclear Medicine.* 2006;36:228-247.

2. Krenning EP, Kwekkeboom DJ, Bakker WH, et al. Somatostatin receptor scintigraphy with In-111-DTPA-D-PHE(1) and I-123-TYR(3)-octreotide - the Rotterdam experience with more than 1000 patients. *European Journal of Nuclear Medicine.* 1993;20:716-731.

3. Gabriel M, Decristoforo C, Donnemiller E, et al. An intrapatient comparison of Tc-99m-EDDA/HYNIC-TOC with In-111-DTPA-octreotide for diagnosis of somatostatin receptor-expressing tumors. *Journal of Nuclear Medicine.* 2003;44:708-716.

4. Gabriel M, Decristoforo C, Kendler D, et al. Ga-68-DOTA-Tyr(3)-octreotide PET in neuroendocrine tumors: Comparison with somatostatin receptor scintigraphy and CT. *Journal of Nuclear Medicine.* 2007;48:508-518.

5. Hofmann M, Maecke H, Borner AR, et al. Biokinetics and imaging with the somatostatin receptor PET radioligand Ga-68-DOTATOC: preliminary data. *European Journal of Nuclear Medicine.* 2001;28:1751-1757.

6. Kowalski J, Henze M, Schuhmacher J, Macke HR, Hofmann M, Haberkorn U. Evaluation of positron emission tomography imaging using [68Ga]-DOTA-D Phe(1)-Tyr(3)-Octreotide in comparison to [111In]-DTPAOC SPECT. First results in patients with neuroendocrine tumors. *Mol Imaging Biol.* 2003;5:42-48.

7. Anderson CJ, Pajeau TS, Edwards WB, Sherman ELC, Rogers BE, Welch MJ. In-Vitro and in-vivo evaluation of copper-64-octreotide conjugates. *Journal of Nuclear Medicine.* 1995;36:2315-2325.

8. Forster GJ, Engelbach M, Brockmann J, et al. Preliminary data on biodistribution and dosimetry for therapy planning of somatostatin receptor positive tumours: comparison of Y-86-DOTATOC and In-111-DTPA-octreotide. *European Journal of Nuclear Medicine.* 2001;28:1743-1750.

9. Jamar F, Barone R, Mathieu I, et al. Y-86-DOTA(0)-D-Phe(1)-Tyr(3)-octreotide (SMT487) - a phase 1 clinical study: pharmacokinetics, biodistribution and renal protective effect of different regimens of amino acid co-infusion. *European Journal of Nuclear Medicine and Molecular Imaging.* 2003;30:510-518.

10. van Essen M, Sundin A, Krenning EP, Kwekkeboom DJ. Neuroendocrine tumours: the role of imaging for diagnosis and therapy. *Nature Reviews Endocrinology.* 2014;10:102-114.

11. Antunes P, Ginj M, Zhang H, et al. Are radiogallium-labelled DOTA-conjugated somatostatin analogues superior to those labelled with other radiometals? *European Journal of Nuclear Medicine and Molecular Imaging.* 2007;34:982-993.

12. Reubi JC, Schar JC, Waser B, et al. Affinity profiles for human somatostatin receptor subtypes SST1-SST5 of somatostatin radiotracers selected for scintigraphic and radiotherapeutic use. *European Journal of Nuclear Medicine.* 2000;27:273-282.

13. Heppeler A, Andre JP, Buschmann I, et al. Metal-ion-dependent biological properties of a chelator-derived somatostatin analogue for tumour targeting. *Chemistry-a European Journal.* 2008;14:3026-3034.

14. Thisgaard H, Olesen ML, Dam JH. Radiosynthesis of Co-55- and Co-58m-labelled DOTATOC for positron emission tomography imaging and targeted radionuclide therapy. *Journal of Labelled Compounds & Radiopharmaceuticals.* 2011;54:758-762.

15. Thisgaard H, Olsen BB, Dam JH, Bollen P, Mollenhauer J, Hoilund-Carlsen PF. Evaluation of Cobalt-Labeled Octreotide Analogs for Molecular Imaging and Auger Electron-Based Radionuclide Therapy. *Journal of Nuclear Medicine.* 2014;55:1311-1316.

16. Pfeifer A, Knigge U, Mortensen J, et al. Clinical PET of Neuroendocrine Tumors Using Cu-64-DOTATATE: First-in-Humans Study. *Journal of Nuclear Medicine.* 2012;53:1207-1215.

17. Thisgaard H, Elema DR, Jensen M. Production and dosimetric aspects of the potent Auger emitter Co-58m for targeted radionuclide therapy of small tumors. *Medical Physics.* 2011;38:4535-4541.

18. Kirschner A, Ice RD, Beierwaltes WH. RADIATION-DOSIMETRY OF I-131-19-IODOCHOLESTEROL. *Journal of Nuclear Medicine.* 1973;14:416-416.

19. Basic anatomical and physiological data for use in radiological protection: reference values. A report of age- and gender-related differences in the anatomical and physiological characteristics of reference individuals. ICRP Publication 89. *Ann ICRP.* 2002;32:5-265.

20. Siegel JA, Thomas SR, Stubbs JB, et al. MIRD pamphlet no. 16: Techniques for quantitative radiopharmaceutical biodistribution data acquisition and analysis for use in human radiation dose estimates. *Journal of Nuclear Medicine.* 1999;40:37S-61S.

21. Stabin MG, Sparks RB, Crowe E. OLINDA/EXM: The second-generation personal computer software for internal dose assessment in nuclear medicine. *Journal of Nuclear Medicine.* 2005;46:1023-1027.

22. Johnbeck CB, Knigge U, Loft A, et al. Head-to-Head Comparison of Cu-64-DOTATATE and Ga-68-DOTATOC PET/CT: A Prospective Study of 59 Patients with Neuroendocrine Tumors. *Journal of Nuclear Medicine.* 2017;58:451-457.

23. Pfeifer A, Knigge U, Binderup T, et al. Cu-64-DOTATATE PET for Neuroendocrine Tumors: A Prospective Head-to-Head Comparison with In-111-DTPA-Octreotide in 112 Patients. *Journal of Nuclear Medicine.* 2015;56:847-854.

24. Junde H. Nuclear data sheets for A=55. *Nuclear Data Sheets.* 2008;109:787-+.

25. Singh B. Nuclear data sheets for A=64. *Nuclear Data Sheets.* 2007;108:197-+.

26. Braad PEN, Hansen SB, Thisgaard H, Hoilund-Carlsen PF. PET imaging with the non-pure positron emitters: Co-55, Y-86 and I-124. *Physics in Medicine and Biology.* 2015;60:3479-3497.

27. Sandstrom M, Velikyan I, Garske-Roman U, et al. Comparative Biodistribution and Radiation Dosimetry of Ga-68-DOTATOC and Ga-68-DOTATATE in Patients with Neuroendocrine Tumors. *Journal of Nuclear Medicine.* 2013;54:1755-1759.

28. Waldvogel-Abramowski S, Waeber G, Gassner C, et al. Physiology of Iron Metabolism. *Transfusion Medicine and Hemotherapy.* 2014;41:213-221.

29. Pagani M, StoneElander S, Larsson SA. Alternative positron emission tomography with non-conventional positron emitters: effects of their physical properties on image quality and potential clinical applications. *European Journal of Nuclear Medicine.* 1997;24:1301-1327.

30. Paans AMJ, Jansen HML. Dose contribution from iron-55 as a daughter radionuclide of cobalt-55. *European Journal of Nuclear Medicine.* 1998;25:445-445.

31. Banerjee SR, Pullambhatla M, Foss CA, et al. Cu-64-Labeled Inhibitors of Prostate-Specific Membrane Antigen for PET Imaging of Prostate Cancer. *Journal of Medicinal Chemistry.* 2014;57:2657-2669.

32. Garrison JC, Rold TL, Sieckman GL, et al. In vivo evaluation and small-animal PET/CT of a prostate cancer mouse model using Cu-64 bombesin analogs: Side-by-side comparison of the CB-TE2A and DOTA chelation systems. *Journal of Nuclear Medicine.* 2007;48:1327-1337.

33. Cui C, Hanyu M, Hatori A, et al. Synthesis and evaluation of Cu-64 PSMA-617 targeted for prostate-specific membrane antigen in prostate cancer. *American Journal of Nuclear Medicine and Molecular Imaging.* 2017;7:40-52.

34. Kanthan GL, Schembri GP, Samra J, Roach P, Hsiao E. Metastatic Renal Cell Carcinoma in the Thyroid Gland and Pancreas Showing Uptake on Ga-68 DOTATATE PET/CT Scan. *Clinical Nuclear Medicine.* 2016;41:583-584.

35. Reubi JC, Kvols L. Somatostatin receptors in human renal-cell carcinomas. *Cancer Research.* 1992;52:6074-6078.

36. Hoog A, Kjellman M, Mattsson P, Juhlin CC, Shabo I. Somatostatin Receptor Expression in Renal Cell Carcinoma-A New Front in the Diagnostics and Treatment of Renal Cell Carcinoma. *Clinical Genitourinary Cancer.* 2018;16:E517-E520.

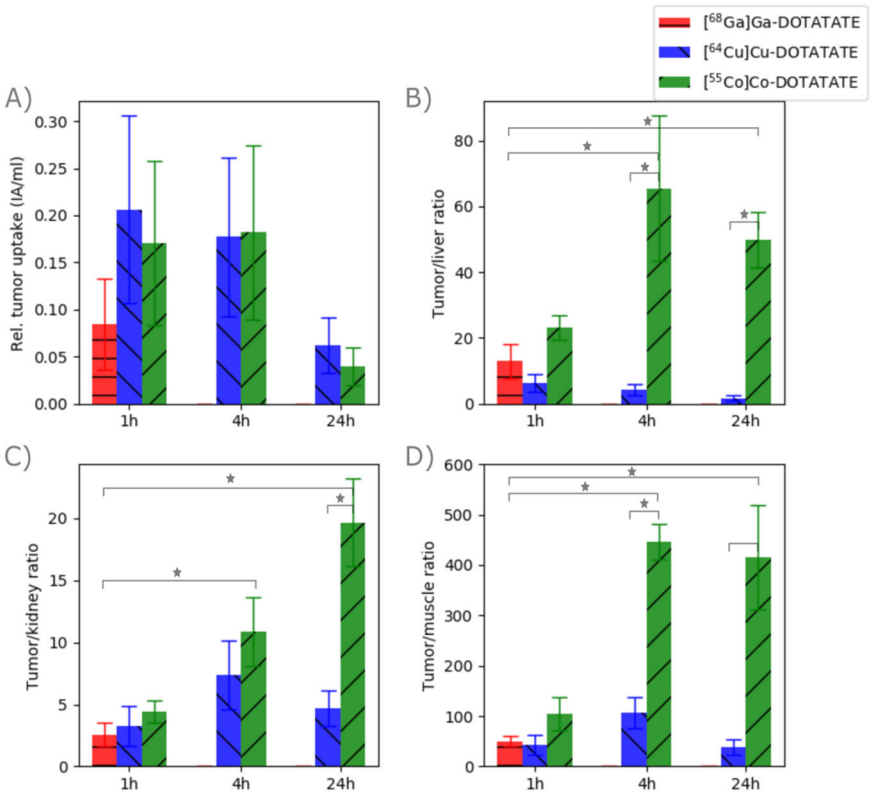

FIGURE 1: Tumor uptake and ratios to liver, kidneys and muscle with standard deviation error bars. Statistical significance ($p < 0.001$) is indicated by stars. No significant difference in tumor uptake was observed while statistically significant differences were found between the three radioconjugates in all tumor to normal tissue ratios. [^{55}Co]Co-DOTATATE showed the highest ratio in liver, kidneys and muscle and showed the highest tumor/liver and tumor/muscle ratio at 4 h p.i.

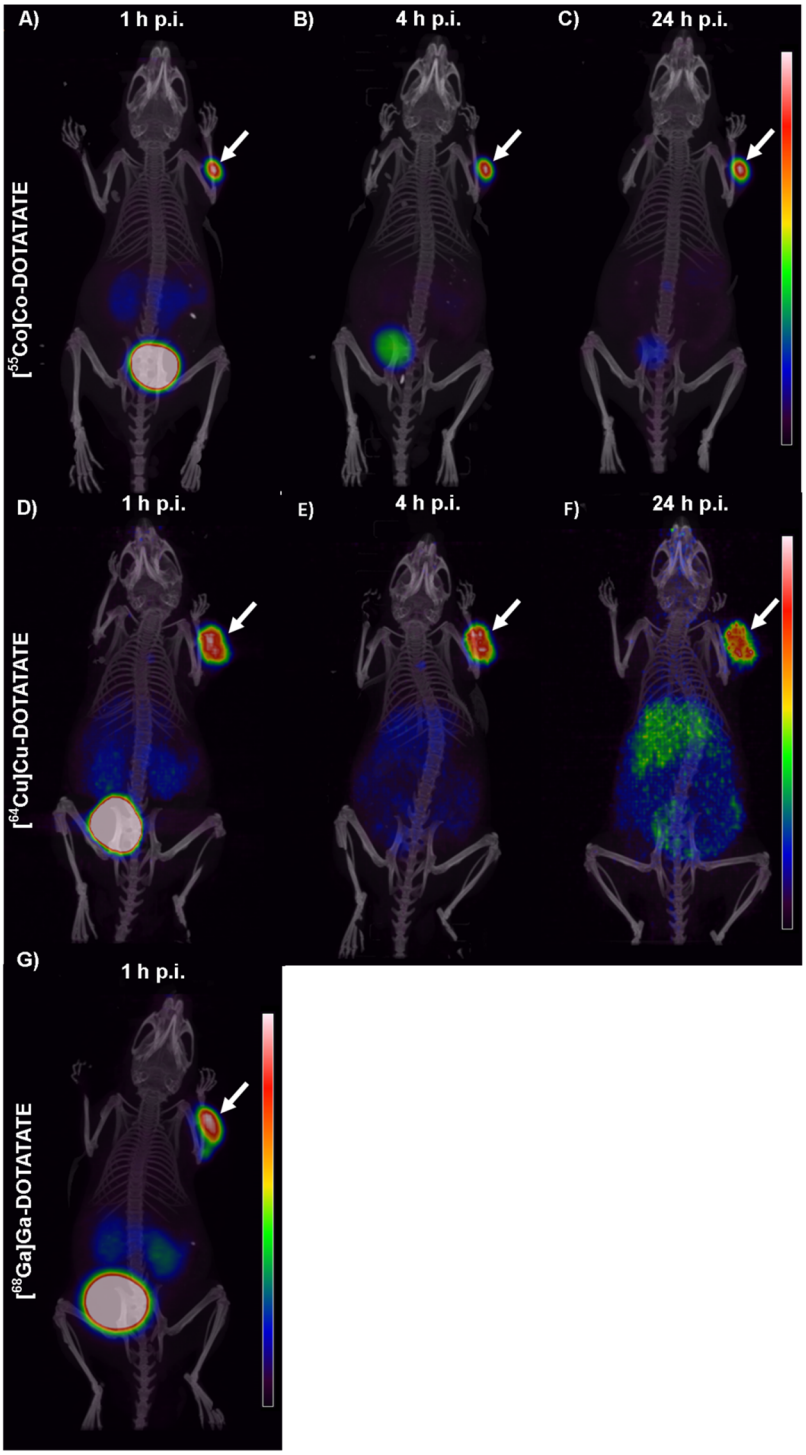

FIGURE 2: Representative maximum intensity projection from the PET/CT scans comparing [^{55}Co]Co-DOTATATE, A) - C), [^{64}Cu]Cu-DOTATATE, D) - F), and [^{68}Ga]Ga-DOTATATE, G). A white arrow indicates the tumor in each animal. A decrease in background was observed for [^{55}Co]Co-DOTATATE for late time point imaging. Oppositely, a higher relative liver uptake with time was observed for [^{64}Cu]Cu-DOTATATE while a high bladder uptake was observed for [^{68}Ga]Ga-DOTATATE. All images are scaled to the maximum uptake in the tumor.

TABLE 1: [^{55}Co]Co-DOTATATE dosimetry results scaled to an adult human from a Co-DOTATATE biodistribution. Largest contributions to the total dose are from the lungs, stomach and liver, respectively.

Organ	$\widetilde{A}_{h,o}$ (hrs)	Effective dose (mSv/MBq)
Adrenals	0.002	3.2E-04
Kidneys	0.12	7.2E-04
Small intestine	0.13	2.8E-04
Liver	0.013	1.2E-03
Lungs	1.77	6.5E-02
Spleen	0.006	2.0E-04
Pancreas	0.03	6.5E-04
Stomach	0.24	2.1E-02
Effective dose		**9.6E-02**

SUPPLEMENTAL TABLE 1: Tumor to target uptakes for the three radioconjugates at 1 h p.i., 4 h p.i. and 24 h p.i., respectively.

	[^{68}Ga]Ga-DOTATATE	[^{64}Cu]Cu-DOTATATE			[^{55}Co]Co-DOTATATE		
	1 h p.i	1 h p.i	4 h p.i.	24 h p.i.	1 h p.i	4 h p.i.	24 h p.i.
Tumor uptake (IA/ml)	0.08±0.04	0.21±0.1	0.18±0.1	0.06±0.02	0.17±0.1	0.18±0.1	0.04±0.02
Tumor/liver ratio	13±5.3	6.3±2.8	4.3±1.8	1.7±0.8	23±4	65±16	50±6
Tumor/kidney ratio	2.5±0.9	3.3±1.6	7.4±2.8	4.7±1.4	4±16	11±16	20±16
Tumor/muscle ratio	50±10	43±20	107±30	38±15	104±16	446±16	414±16